In-gas-cell laser ionization studies of plutonium isotopes at IGISOL

I. Pohjalainen[a,*], I.D. Moore[a,*], T. Kron[b], S. Raeder[c,d], V. Sonnenschein[e], H. Tomita[e], N. Trautmann[f], A. Voss[a], K. Wendt[b]

[a]*University of Jyvaskyla, Department of Physics, P.O. Box 35 (YFL), FI-40014 University of Jyvaskyla, Finland*
[b]*Institut für Physik, Johannes Gutenberg Universität, 55128 Mainz, Germany*
[c]*Helmholtz-Institut Mainz, 55128, Mainz, Germany*
[d]*KU Leuven, Instituut voor Kern- en Stralingsfysica, B-3001 Leuven, Belgium*
[e]*Nagoya University, Furo-cho, Chikusa-ku, Nagoya, 464-8603, Japan*
[f]*Institute of Nuclear Chemistry, University of Mainz, Fritz-Straßmann-Weg 2, 55128 Mainz, Germany*

Abstract

In-gas-cell resonance laser ionization has been performed on long-lived isotopes of Pu at the IGISOL facility, Jyväskylä. This initiates a new programme of research towards high-resolution optical spectroscopy of heavy actinide elements which can be produced in sufficient quantities at research reactors and transported to facilities elsewhere. In this work a new gas cell has been constructed for fast extraction of laser-ionized elements. Samples of $^{238-242}$Pu and ^{244}Pu have been evaporated from Ta filaments, laser ionized, mass separated and delivered to the collinear laser spectroscopy station. Here we report on the performance of the gas cell through studies of the mass spectra obtained in helium and argon, before and after the radiofrequency quadrupole cooler-buncher. This provides valuable insight into the gas phase chemistry exhibited by Pu, which has been additionally supported by measurements of ion time profiles. The resulting monoatomic yields are sufficient for collinear laser spectroscopy. A gamma-ray spectroscopic analysis of the Pu samples shows a good agreement with the assay provided by the Mainz Nuclear Chemistry department.

Keywords: Resonance laser ionization, gas phase chemistry, gas cell, plutonium

1. Introduction

The actinide elements cover the atomic number range from Ac (Z=89) to Lr (Z=103), beyond which lie the superheavy elements. It is this region which poses some of the most difficult and yet exciting challenges to experimentalists, requiring highly sensitive techniques to make efficient use of the limited quantity of isotopes which can be produced. Nuclear structure information obtained from optical spectroscopy is limited, in particular above Ra (Z=88) which corresponds to the last isotopic chain for which collinear laser spectroscopy has been performed [1]. This reflects a combination of low production cross sections coupled with a lack of stable isotopes, thus only limited knowledge of optical transitions. Traditionally, actinide spectroscopy has been motivated by atomic energy level analysis, with more recent techniques including resonance ionization mass spectrometry applied to determine fundamental atomic properties such as the ionization potential [2]. Probing the evolution of shell structure and the development of nuclear deformation of the heaviest elements using model-independent laser spectroscopic techniques is a current goal at a number of facilities. It is clear that a step-wise approach will be needed to successfully produce the requisite radioactive beams, including characterisation of optical transitions for selective and efficient ionization. Further studies will then be required in order to optimize the optical spectroscopy for high-resolution measurements.

Recently, a new programme to study heavy elements using a combination of laser resonance ionization and collinear laser spectroscopy has been initiated at the IGISOL facility, in the Accelerator Laboratory of the University of Jyväskylä. Several elements above Ra have long-lived isotopes for which sufficiently large sample sizes (ng) of material can be produced at nuclear reactors and safely transported to facilities for nuclear structure studies. In collaboration with the Nuclear Chemistry department of the University of Mainz, samples containing Pu isotopes ($^{238-242}$Pu and ^{244}Pu) were electrolytically deposited onto a tantalum substrate and delivered to Jyväskylä. After electrothermally heating the filament inside a gas cell filled with helium or argon, in-gas-cell resonance laser ionization was applied to selectively ionize the plutonium. The yield of the Pu^+ ionic fraction was sufficient to perform high-resolution collinear laser spectroscopy. The high resolution data is currently under analysis and will be published elsewhere.

In this article preliminary investigations of a new gas cell for off-line heavy element laser ionization will be presented. A careful analysis of resulting mass spectra using the IGISOL separator has been performed in combination with studies of the ion time profiles following laser ionization with pulsed lasers. Such information is of importance to understand the timescales associated with molecular formation during extraction of the Pu^+ ions from the gas cell. In light of these studies, new modifications are planned to further improve the yield of the ele-

*Corresponding author.
Email addresses: ilkka.pohjalainen@jyu.fi (I. Pohjalainen), iain.d.moore@jyu.fi (I.D. Moore)

ment of interest in the form of singly-charged monoatomic ions which directly impacts the sample sizes required for collinear laser spectroscopy. Finally the results of a gamma-ray spectroscopy analysis of one of the plutonium samples is presented, performed in a low-background counting station. This has allowed a direct comparison with the original sample assay provided by Mainz.

2. Development of a new gas cell and ionization of Pu

The application of gas cell laser ionization at IGISOL was originally motivated by the goal of improving the rather modest efficiency (∼1%) of the heavy-ion fusion-evaporation ion guide (HIGISOL) as well as recognizing the need to move towards a more element-selective approach in the production of radioactive ion beams. A number of considerations were taken into account in the design of the gas cell including efficient evacuation of a large recoil stopping volume (optimized gas flow transport and exit nozzle type), water cooling and baking capabilities, and optional filament feedthroughs as well as dc electrodes. This resulted in a modular construction consisting of a gas feeding part, the main body (with optional filament holder) and a removable exit nozzle/hole [3]. The volume of the main body to the exit hole of ∼250 cm^3 resulted in an evacuation time of 390 ms for a standard 1.2 mm diameter exit hole using helium as buffer gas.

In order for the successful extraction of atomic ions, the requirement for conditions of high gas purity (sub parts-per-billion) has been critical to the success of so-called laser ion guides as well as large gas catchers due to the competition between atomic ion survival against molecular formation and evacuation timescales. For several of the refractory elements that can only be produced with the gas cell method, the reaction rate coefficients which govern the time evolution of molecular formation indicate extremely strong affinity with the main buffer gas contaminants, water and oxygen [4]. In on-line conditions, the critical loss mechanism for an ion of interest is that of neutralization within the high density of (primarily) buffer gas ion-electron pairs created by the passage of a primary projectile beam. The operational principal of laser ionization in a gas cell takes advantage of this fast ion-electron recombination, with re-ionization applied in a volume where the ion-electron density is sufficiently low for a high chance of survival of the photo-ions. One can understand that the operation of the gas cell is strongly dependent on a set of competing time scales. By studying the time distribution profiles of (mass separated) ions one is able to determine the effective volume for laser ionization within the gas cell. At the Leuven laser ion source (LISOL) it was shown that at time scales of approximately 5 ms, recombination losses start to gain importance above an ion-electron density of 10^7-10^8 pairs/cm^3 [5, 6]. At IGISOL, similar experiments verified that the accessible neutral fraction in the presence of a primary beam is restricted to the nozzle region, an effective laser ionization volume which is evacuated within milliseconds [7].

The current programme focuses on heavy element studies not requiring the presence of a primary beam. Therefore, much of the gas cell volume necessitated by the stopping distribution of heavy-ion fusion-evaporation recoils is redundant. Long-lived isotopes of actinide elements including plutonium and thorium can be prepared onto substrates for subsequent evaporation into a volume which may be minimized to reduce possible molecular formation or other loss mechanisms such as diffusion to the walls of the gas cell. Ideally, such a volume is limited only by the efficiency of the laser ionization process. Assuming that an atom can be ionized by a single laser pulse and requiring that every atom is irradiated at least once by the lasers, the minimum volume V_{min} is set by the repetition rate of the laser system and the conductance C of the gas cell,

$$V_{min} = t_{rep} C = t_{rep} \cdot 0.45 \cdot \phi^2, \quad (1)$$

where t_{rep} is the time between the laser pulses and the conductance C has been given in terms of the exit hole diameter ϕ in mm for the case of room temperature helium. Considering the 10 kHz repetition rate of the Ti:sapphire laser system used at IGISOL and with a typical exit hole size ϕ = 1.2 mm, Eq. 1 results in a volume of 0.07 cm^3. However, the assumption that an atom would be ionized by a single laser pulse is unrealistic for a high repetition rate (10 kHz) laser system where the energy per pulse of the fundamental radiation can be a factor of ten lower compared to a medium repetition rate (200 Hz) system. In order for a laser system with a single pulse laser ionization efficiency ϵ_p to result in a total laser ionization efficiency > 80%, the minimum volume defined by Eq. 1 must be scaled by the factor $-2/\ln(1-\epsilon_p)$.

Currently we have no available data on the single pulse laser ionization efficiency at IGISOL, however a recent experiment at LISOL compared the performance of a similar high repetition rate Ti:sapphire laser system with the medium repetition rate dye laser system in studies of copper and cobalt [8]. In that work, by controlling the synchronization of the Ti:sapphire laser pulses, it was possible to match the repetition rates of both laser systems without affecting the energy per pulse of the Ti:sapphire laser. Whereas the dye laser system could saturate the atomic transitions and was seen to saturate the ion signal at ∼100 Hz (corresponding to an irradiated volume representing ∼40% of the total volume of the ionization chamber, evacuated in about 10 ms), the Ti:sapphire system was unable to saturate all transitions. Furthermore, when operated at the same repetition rate the ionization efficiency was around 200 times smaller. Ferrer and colleagues use this factor to infer an efficiency per pulse of 0.5% for the Ti:sapphire system in those experiments. This value can be inserted into our scaling factor and when multiplied by the minimum volume results in a required ionization volume of ∼30 cm^3. We note that by strongly focusing the Ti:sapphire beams in the LISOL experiment the ionization efficiency per pulse was increased to such an extent that the two laser systems performed comparably under on-line conditions.

The gas cell design in the current work was primarily motivated by the wish to reduce the redundant HIGISOL volume while being restricted by the practical consideration to reuse the same filament holder. An additional motivation for a dedi-

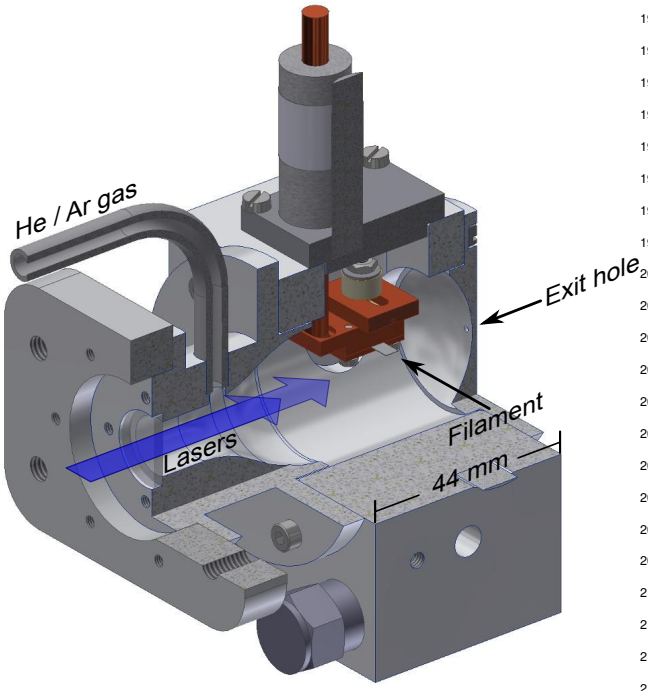

Figure 1: Cross-sectional view of the gas cell used for heavy element studies with the filament in place.

cated gas cell took into account the expected surface contamination with long-lived alpha-active isotopes when using actinide sources. Figure 1 presents a cross-sectional view of the gas cell. Helium or argon buffer gas is fed through an inlet tube into the cell which has a volume of ~30 cm^3. This volume of gas, which is kept at a pressure of ~70 mbar, is extracted through a 1.2 mm exit hole into a chamber maintained at a pressure of ~10^{-2} mbar. With a such a pressure difference the gas flow is choked and thus the conductance is pressure independent. An evacuation time for the whole gas cell volume of ~50 ms and ~150 ms can be estimated for room temperature helium and argon, respectively, for any operational pressure. Laser radiation is introduced through a sapphire window mounted on the rear of the gas cell, directed along the extraction axis of the cell very close (~1 mm) to the filament. This geometry was designed to maximise the laser overlap with the highest density of atoms following evaporation from the filament. Additional elements include a heater cartridge added for in-situ baking, water cooling, and the possibility to insert windows and targets for future introduction of a primary beam.

In total, six filaments (with dimensions 11 mm × 3.5 mm, and thickness 50 µm) were provided from the Nuclear Chemistry department of Mainz. Two of the filaments were blank and were used for testing purposes in order to understand the behaviour of the voltage across the feedthroughs on the target chamber as a function of the current applied to the filament, to measure the temperature of the filament with a pyrometer as a function of current (and, at a fixed current, the temperature as a function of gas pressure) and to search for surface ions which could be used to calibrate the magnetic field of the mass separator. The other four samples contained a mixture of Pu isotopes with up to ~10^{16} atoms for the most abundant isotope ^{244}Pu, to ~10^{12} atoms for ^{238}Pu. Two of the four samples also contained ^{239}Pu and were used specifically in connection with the high-resolution laser spectroscopy experiment. In the current work however we focus only on the samples without ^{239}Pu. To prevent oxidation of the plutonium, the samples were covered with an additional protective Ti layer of about 1 μm on the surface.

During operation the filaments were heated to a temperature of typically 1000-1200°C depending on the desired release rate of the Pu atoms. Variations in gas pressure affected the temperature and thus the evaporation rate. For a measured current of 28A (heating power 99 W), an increase of helium pressure from 50 mbar to 150 mbar resulted in a corresponding temperature decrease from 1050°C to 950°C.

Initially a three-step ionization scheme using laser radiation at wavelengths of 420.76, 847.26, and 750.24 nm was chosen based on trace analysis studies by Raeder *et al* [9] . In that work a full saturation of all optical excitation steps was demonstrated ensuring a high efficiency of the ionization process. At IGISOL the laser light was provided by three broadband Ti:sapphire lasers, the characteristics of which can be found elsewhere [10]. In the gas cell however little or no indication of the effect of the second and third IR steps was seen and it was suspected that the excitation preferentially proceeded via a Rydberg state populated by a photon from the first step transition which was subsequently ionized via buffer gas collisions. Indications for such an effect could be clearly observed in the saturation behaviour of the first step. A second laser was therefore introduced operating in the blue wavelength regime, both lasers using intracavity second harmonic generation (SHG) [11]. The first step laser, tuned to a wavelength of 420.76 nm, corresponds to a transition from the 5f^{6}7s^2 $^7F_0$ ground state to an excited state at 23766.14 cm^{-1} with configuration 5f^{6}7s7p $^7D_1$. The wavelength of the second step laser was optimised to a resonance observed at a wavelength of 422.53 nm. Further studies showed that the two transitions are able to ionize independently from one another (though with much reduced count rates), which may be explained if the second step is driving population from the lowest-lying metastable state at 2203.61 cm^{-1} to a state at 25870.69 cm^{-1}. It is of interest for further work to determine whether this state is naturally populated due to the temperature of the hot filament. Nevertheless, ionization will proceed via Rydberg states populated following excitation from the 23766.14 cm^{-1} level, and/or non-resonantly or to auto-ionizing states if a second path proceeds via the state at 25870.69 cm^{-1}.

Surprisingly, it was seen that the Pu$^+$ ion count rate was maximised when both of the Ti:sapphire lasers were operated without the etalons in the resonator cavity. This increases the fundamental linewidth from 4-5 GHz to ~100 GHz, or approximately 0.2 nm at a wavelength of 840 nm. The resulting laser linewidth is considerably larger than the atomic linewidth contributions from Doppler and pressure broadening resulting in a lower spectral power density. Nevertheless, the loss in spectral power density may be offset if we are strongly saturating the transition, which is indeed the case for the first step. The modest increase in laser power without the etalon, coupled with the

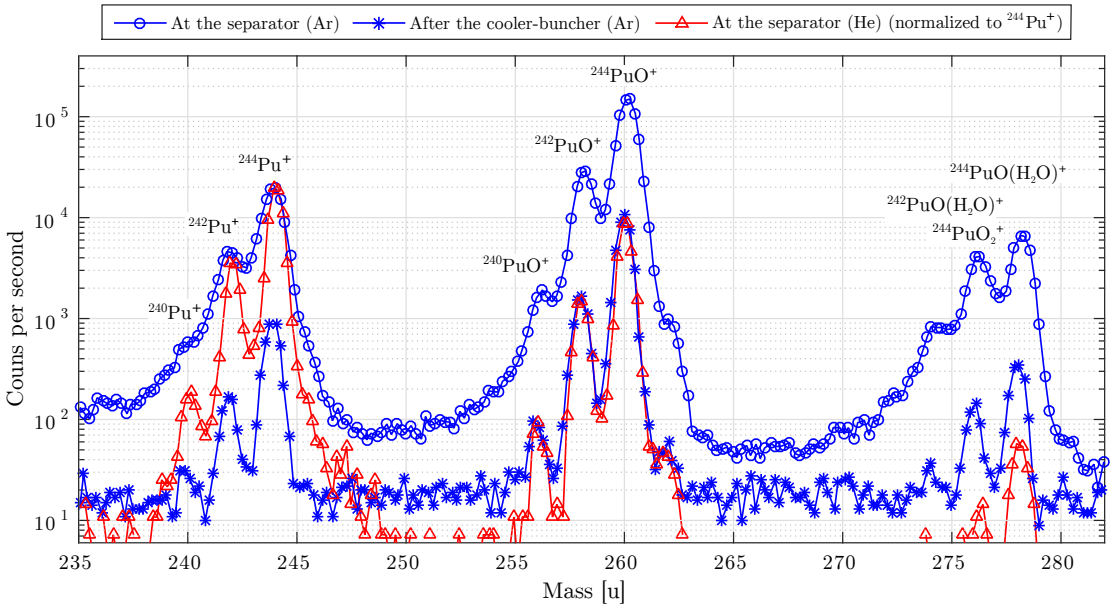

Figure 2: Mass spectra in the region of Pu and related molecules recorded at the focal plane of the IGISOL separator using He and Ar buffer gases and after the cooler-buncher (argon only). See text for details. Colour on-line.

simultaneous population of a number of Rydberg states can explain the higher ion count rate. In order to better understand the ionization process and to scan for Rydberg levels exhibiting a higher ionization cross section, further investigation is required.

3. Gas phase chemistry

The cleanliness of the buffer gas and gas cell was characterized by recording mass spectra (Fig. 2) with a microchannel plate (MCP) detector at the focal plane of the IGISOL mass separator using both He and Ar buffer gases at a pressure of ~75 mbar. Additionally, a mass spectrum was taken using Ar with a MCP detector situated at the end of the collinear laser line located after the radiofrequency (rf) cooler-buncher. This provided additional insight on the effect of the cooler-buncher on the mass spectra and also confidence in transporting Pu^+ ions to the laser spectroscopy station. All of the spectra show an isotopic abundance pattern that matches the isotope assay of the samples provided by Mainz, both in the region of singly-charged monoatomic ions and also at higher masses identified with molecular formation of Pu^+ ions. The transport efficiency through the separator system is believed to be rather constant in this mass range.

The first molecular isotopic pattern is observed 16 mass units heavier than the monoatomic pattern and corresponds to PuO^+ ions. There are two possible pathways to oxidize plutonium considering H_2O and O_2 are two of the main impurities in the gas:

$$Pu^+ + O_2 \longrightarrow PuO^+ + O, \quad k_2 = 1.5 \cdot 10^{-10}\ \mathrm{cm^3/s} \quad (2a)$$

$$Pu^+ + H_2O \longrightarrow PuO^+ + H_2, \quad k_2 = 7 \cdot 10^{-12}\ \mathrm{cm^3/s}. \quad (2b)$$

For both reactions, the bimolecular reaction rate k_2 has been calculated from experimental values of reaction efficiencies, or the k_2/k_{ADO} values, measured by Santos *et al* [12]. The accuracy of these values is estimated to be ±50%. The average dipole orientation collisional rate, k_{ADO}, was calculated as follows,

$$k_{ADO} = \frac{2\pi q}{\sqrt{\mu}}\left(\sqrt{\alpha} + c\mu_D\sqrt{\frac{2}{\pi kT}}\right), \quad (3)$$

where q is the charge of the ion and μ is the reduced mass [13]. The factor c is the locking constant, α and μ_D are the polarizibility and the permanent dipole of the reagent molecule, respectively, all values of which have been taken from Table 7.1 and Fig. 7.1 in Ref. [14].

After formation, the PuO^+ ions can react further with water molecules in a termolecular association reaction:

$$PuO^+ + H_2O + M \longrightarrow PuO(H_2O)^+ + M, \quad (4)$$

where M is a buffer gas atom. This association reaction accounts for the peaks 34 mass units above the monoatomic Pu^+ ions. In Ar there also appears to be oxidation of the PuO^+ through similar reactions as in Eqs (2a) and (2b) because the count rate at $(M/q) = 276$ is higher than one would expect from the isotopic ratios.

Even though both helium and argon gases are purified with the IGISOL rare gas purification system [15] and both the gas cell and gas lines are baked before an experiment, the purity conditions appear to be unusually poor. This can be inferred from the large amount of molecular formation as seen in Fig. 2. Assuming molecular formation as discussed, the time constant associated with the process can be defined using $\tau = 1/k_2[M]$, where M is the impurity concentration. With an expected impurity level of 1 ppb of purified gas, the Pu^+ ion survival time

τ		Helium	Argon
Rising	Pu^+	0.80 ± 0.05 ms	2.57 ± 0.16 ms
	PuO^+	1.17 ± 0.09 ms	3.25 ± 0.07 ms
Falling	Pu^+	1.13 ± 0.04 ms	6.96 ± 0.15 ms
	PuO^+	1.14 ± 0.05 ms	6.75 ± 0.07 ms

Table 1: Time parameter τ for rising and falling edges of the Pu^+ and PuO^+ ion signal time profiles illustrated in Fig. 3 for helium and argon.

is in order of a few seconds, a timescale much longer than the evacuation time of the gas cell. We therefore suspect that additonal impurities result from an unfortunate "dead" volume in the filament holder, which could have trapped some air, or to outgassing of the gas cell while the filament is being heated.

The most notable difference between the mass spectra obtained using helium and argon is the lower mass resolution in the case of argon. This is a reflection of collisions between buffer gas atoms and ions in the extraction region after the gas cell which leads to an energy spread, more pronounced in the case of argon because of the heavier mass. With argon, the effect of transporting the beam through the RF cooler-buncher is seen in an improvement in the mass resolving power (as well as a reduction in the count rate due to reduced transmission). This can be understood if the cooler-buncher acceptance window of ~90 eV is considered. Only the part of the mass-separated beam that has the right energy enters the cooler, reducing the peak widths.

4. Study of the dynamic processes within the gas cell

In order to investigate the dynamic processes inside the gas cell following the creation of a photo-ion, the temporal behavior of mass-separated ions was studied by chopping the laser beams with a fast shutter mechanism. The resulting time structure of the ions was recorded with a multi-channel scaler connected to the MCP located at the focal plane of the mass separator. Figure 3 shows an example of the time profiles of Pu^+ and PuO^+ in He and Ar when the lasers were introduced at time t~0 s and turned off at t ~1.13 s. The small peak visible at the start of the time profile of Pu^+ in helium is caused by the initial ion creation in the nozzle region which is evacuated before molecular formation occurs. This is not seen in argon, probably due to the slower evacuation of the gas cell. Exponential growth and decay curves

$$y(t) = \begin{cases} A_0 \pm A\left(1 - e^{-\frac{t-t_0}{\tau}}\right) & \text{if } t \geq t_0 \\ A_0 & \text{if } t < t_0 \end{cases} \quad (5)$$

were fitted to the rising and falling edges of the time profile, respectively, to extract a time parameter τ for each fit. These parameters represent the time scales during which the ion signal develops at the start of a laser pulse and how it decays once the lasers are blocked. Table 1 summarizes the time scales for the data illustrated in Fig. 3

One can immediately note from the fit parameters that in both helium and argon the atomic Pu^+ ions achieve saturation sooner

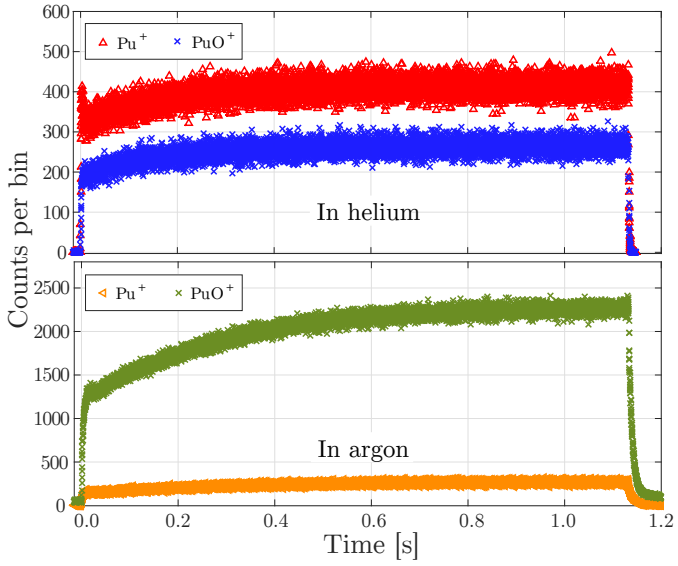

Figure 3: Time distribution profiles of Pu^+ and PuO^+ in He (top) and Ar (bottom). In order to quantify the profiles exponential growth and decay curves were fitted to the rising and falling edges of the distribution in order to determine the different time constants τ, summarized in Table 1. Colour on-line.

than the corresponding PuO^+ molecule. This is to be expected as the oxide can only be produced following laser ionization of the atomic species. The slower time scale in Ar reflects the reduced conductance of the exit hole. It is interesting to note that the time parameters for the falling edges of the profiles are somewhat longer than the rising edges and both the atomic and molecular species have the same fit parameter within errors. This likely reflects the fact that both species are extracted from the same effective volume.

In all cases τ is notably lower than the total evacuation time of the gas cell indicating a fast loss mechanism of the plutonium (and its corresponding oxide). The alpha particles emanating from the samples in the radioactive decay of Pu are estimated to create an ionization density rate in He, $Q = 10^5$ ion-electron pairs $cm^{-3}s^{-1}$, which is negligible if one were to consider recombination losses due to free electrons. In addition, charge exchange between the Pu^+ ions and buffer gas atoms or typical gas impurities is not possible because of the low ionization potential of Pu. The only conceivable loss mechanisms of the ions are molecular formation and diffusion losses to the walls of the gas cell. The information gained from the mass spectra in Fig. 2 indicates a source of impurities which is independent of whether He or Ar is used and we believe this to be caused by the filament holder as previously mentioned.

Using the known conductance of the exit hole, the time parameter τ translates into an effective volume for laser ionization. This effective volume will be different depending on whether one chooses to use the rising or falling edge of the Pu^+ ion time distribution. We have chosen to use the falling edge as the starting conditions are different to the situation before laser ionization has commenced; all competing processes which create and destroy the ion of interest are in equilibrium. By taking into account the different conductances of the gas cell in He and

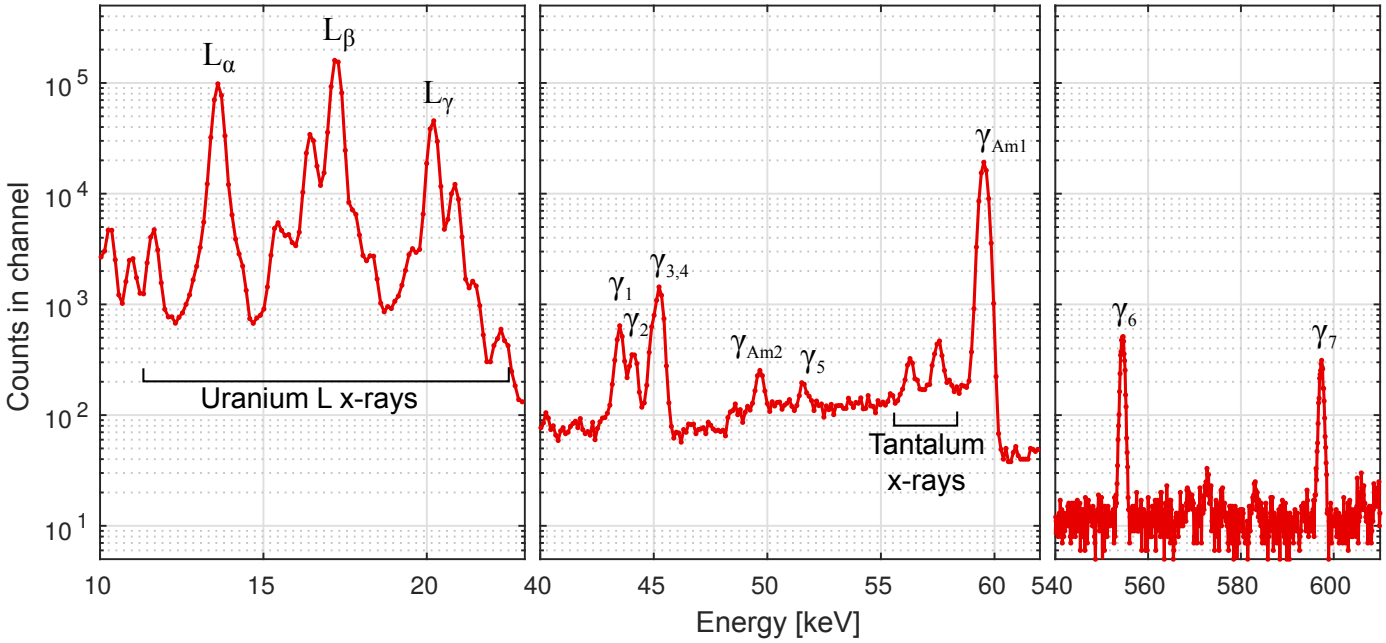

Figure 4: A gamma spectrum from an unused Pu sample. Three energy regions of interest are highlighted. In addition to the gamma radiation associated with the decay of Pu, the spectrum contains low energy X-rays, an ^{241}Am contaminant and X-rays of Ta, the material from which the filament is made.

Peak	Energy (keV)	Isotope branching (%) ^{238}Pu [16]	^{239}Pu [17]	^{240}Pu [17]	^{242}Pu [18]	Activity (Bq)
L_α	13.6	3.81(3)	1.65(4)	3.73(5)	3.2(2)	1130
L_β	17.22	4.26(3)	1.72(4)	3.95(6)	3.4(3)	1050
L_γ	20.2	0.992(7)	0.428(14)	0.95(2)	0.79(9)	1165

Table 2: The three uranium x-rays peaks that were used to determine the total activity of a plutonium filament. In addition to peak energies and activities the branching to these peaks are given for each isotope in the filament if found in literature.

Ar buffer gases, the effective volume for the ionization of Pu is ~ 0.7 cm^3 in He and ~ 1.4 cm^3 in Ar, which is only a few percent of the total gas cell volume. This indicates that detected monoatomic laser ions are originating not far from the nozzle region. Gas phase chemistry and related ion time profiles using similarly reactive elements have been previously studied in greater detail at IGISOL and in that work the increase in the effective volume due to a reduction of impurities in the gas was clearly observed [19].

5. Gamma ray spectroscopy of the Pu samples

Gamma ray spectroscopy was used to independently analyze the content of a filament, in support of the assay provided by Mainz, and also to have means of monitoring the remaining activity of a partly used filament. The majority of the Pu isotopes in the samples alpha decay directly to the ground state of a long-lived daughter or to a low-lying excited state, which subsequently decays emitting conversion electrons (the branching fraction to decay via gamma radiation is very low, <0.05%). Further difficulties arise in such a measurement because the gamma energies between different isotopes tend to cluster to within ~1 keV or less. However, using a long enough measurement time in a low-background station which is coupled to a low-energy high-purity germanium detector, a gamma spectrum of one unused Pu filament was successfully measured in the range from 3 keV to 800 keV.

Figure 4 shows three regions of interest of the gamma spectrum: the 10-25 keV region containing L X-ray peaks associated with the U daughter; the 40-65 keV region that has the strongest gamma peaks associated with the decay radiation of Pu; a high-energy region around 580 keV showing the gamma rays of ^{240m}Np which is in the decay chain of ^{244}Pu. In addition an ^{241}Am contaminant was detected along with X-rays of Ta induced by the Pu alpha decay in the sample.

The total activity of the Pu isotopes in the filament was determined separately from the three uranium L x-ray peaks using known isotopic abundances from the assay and branching ratios for each peak of each Pu isotope [16, 17, 18]. No information could be found for the branching ratio of these X-rays for ^{244}Pu in the literature however this does not affect the calculation of the total activity as its activity is under 10 Bq. The peak energies, branching ratios and measurement results are summarized in Table 2. The mean value of ~1120 Bq matches well with the stated assay activity of 1154 Bq.

Peak	Energy (keV)	Isotope	Branching (%)	Activity (Bq)	Assay (Bq)
γ_1	43.5	^{238}Pu	0.0392	200	219
γ_2	44.1	^{240}U	1.05	9	7
γ_3	44.9	^{242}Pu	0.0373	160	182
γ_4	45.2	^{240}Pu	0.0447	510	518
γ_5	51.624	^{239}Pu	0.02722	51	228
γ_6	554.49	^{240m}Np	20.9	7	7
γ_7	597.37	^{240m}Np	11.7	7	7
γ_{Am1}	59.532	^{241}Am	35.9	9	-

Table 3: The list of identified gamma rays from the spectrum in Fig. 4 with peak energies and branching ratios [20]. The determined activities of the plutonium isotopes in the filament using these peaks are listed. The activities of ^{240}U and ^{240m}Np can be measured for an indirect determination of the activity of ^{244}Pu. The assay of the filament is listed for comparison.

The individual activities of the Pu isotopes in the sample were determined from the peaks in the 43-52 keV region. Although some peaks overlap, by fitting simple Gaussian functions using the peak width extracted from the ^{241}Am line and the peak energies for each isotope [20], it was possible to obtain the yields for each gamma line. By accounting for the detector efficiency and branching ratio for the gamma rays the activities of the isotopes were calculated (Table 3). The activity of ^{244}Pu was not directly determined because of its low activity however its decay chain contains short-lived ^{240}U and ^{240m}Np having sufficiently strong branching ratios for gamma rays. Thus the activity of ^{244}Pu could be indirectly determined. As seen in Table 3 the individual activities agree well with those provided in the assay except in the case of ^{239}Pu whose measured activity is notably lower. The discrepancy was also seen in the isotopic abundance pattern of the plutonium mass spectrum from a filament containing ^{239}Pu which was made during a later experiment.

6. Conclusion

Long-lived isotopes of Pu provided by the Nuclear Chemsitry department of the University of Mainz were successfully extracted as low-energy ion beams at IGISOL following resonance laser ionization in a He and Ar buffer gas-filled cell. Although further work is required to fully characterize the ionization scheme, a sufficient yield of monoatomic Pu^+ ions was produced in preparation for high-resolution collinear laser spectroscopy. Studies of the mass spectra as well as ion time profiles indicate a source of impurities which is likely due to outgassing of "dead" volumes in the filament holder and perhaps via heating of the filament. A new filament holder is currently being designed to partially address this issue. These successful studies will be continued in the future in order to expand the programme of laser spectrocopy of actinide elements at IGISOL, with immediate interest in ^{229}Th as part of the new EU Horizon 2020 project, NuClock, which is focused on the study of the low-lying isomeric state.

7. Acknowledgements

This work has been supported by the Academy of Finland programme under the Finnish Centre of Excellence Programme 2012-2017 (Project No. 251353, Nuclear and Accelerator-Based Physics Research at JYFL) and the European Commission (E.C.) 7th Framework Programme project ENSAR.

8. References

[1] S. A. Ahmad, W. Klempt, R. Neugart, E. W. Otten, P. G. Reinhard, G. Ulm, K. Wendt, Mean square charge radii of radium isotopes and octupole deformation in the $^{220-228}$Ra region, Nuclear Physics A 483 (2) (1988) 244–268. doi:http://dx.doi.org/10.1016/0375-9474(88)90534-9.

[2] S. Rothe, A. N. Andreyev, S. Antalic, A. Borschevsky, L. Capponi, T. E. Cocolios, H. De Witte, E. Eliav, D. V. Fedorov, V. N. Fedosseev, D. A. Fink, S. Fritzsche, L. Ghys, M. Huyse, N. Imai, U. Kaldor, Y. Kudryavtsev, U. Köster, J. F. W. Lane, J. Lassen, V. Liberati, K. M. Lynch, B. A. Marsh, K. Nishio, D. Pauwels, V. Pershina, L. Popescu, T. J. Procter, D. Radulov, S. Raeder, M. M. Rajabali, E. Rapisarda, R. E. Rossel, K. Sandhu, M. D. Seliverstov, A. M. Sjödin, P. Van den Bergh, P. Van Duppen, M. Venhart, Y. Wakabayashi, K. D. A. Wendt, Measurement of the first ionization potential of astatine by laser ionization spectroscopy, Nat. Commun. 4 (2013) 1835.
URL `http://dx.doi.org/10.1038/ncomms2819`

[3] I. Moore, P. Dendooven, J. Ärje, The IGISOL technique—three decades of developments, Hyperfine Interactions 223 (1-3) (2014) 17–62. doi:10.1007/s10751-013-0871-0.
URL `http://dx.doi.org/10.1007/s10751-013-0871-0`

[4] G. K. Koyanagi, D. Caraiman, V. Blagojevic, D. K. Bohme, Gas-phase reactions of transition-metal ions with molecular oxygen: room temperature kinetics and periodicities in reactivity, J. Phys. Chem. A 106 (2002) 4581.

[5] M. Huyse, M. Facina, Y. Kudryavtsev, P. V. Duppen, I. collaboration, Intensity limitations of a gas cell for stopping, storing and guiding of radioactive ions, Nucl. Instr. and Meth. in Phys. Res. B 187 (2002) 535.

[6] M. Facina, B. Bruyneel, S. Dean, J. Gentens, M. Huyse, Y. Kudryavtsev, P. V. den Bergh, P. V. Duppen, A gas cell for thermalizing, storing and transporting radioactive atoms and ions. Part II: On-line studies with a laser ion source, Nucl. Instr. and Meth. in Phys. Res. B 226 (2004) 401.

[7] I. D. Moore, T. Kessler, T. Sonoda, Y. Kudryavstev, K. Peräjärvi, A. Popov, K. D. A. Wendt, J. Äystö, A study of on-line gas cell processes at IGISOL, Nucl. Instrum. Methods Phys. Res. B 268 (6) (2010) 657 – 670.

[8] R. Ferrer, V. Sonnenschein, B. Bastin, S. Franchoo, M. Huyse, Y. Kudryavtsev, T. Kron, N. Lecesne, I. Moore, B. Osmond, D. Pauwels, D. Radulov, S. Raeder, L. Rens, M. Reponen, J. Roßnagel, H. Savajols, T. Sonoda, J. Thomas, P. V. den Bergh, P. V. Duppen, K. Wendt, S. Zemlyanoy, Performance of a high repetition pulse rate laser system for in-gas-jet laser ionization studies with the leuven laser ion source @ LISOL, Nuclear Instruments and Methods in Physics Research Section B: Beam Interactions with Materials and Atoms 291 (2012) 29 – 37. doi:http://dx.doi.org/10.1016/j.nimb.2012.08.023.

[9] S. Raeder, A. Hakimi, N. Stöbener, N. Trautmann, K. Wendt, Detection of plutonium isotopes at lowest quantities using in-source resonance ionization mass spectrometry, Analytical and Bioanalytical Chemistry 404 (8) (2012) 2163–2172.

[10] M. Reponen, I. D. Moore, T. Kessler, I. Pohjalainen, S. Rothe, V. Sonnenschein, Laser developments and resonance ionization spectroscopy at IGISOL, Eur. Phys. J. A 48 (2012) 45.

[11] V. Sonnenschein, I. D. Moore, I. Pohjalainen, M. Reponen, S. Rothe, K. Wendt, Intracavity Frequency Doubling and Difference Frequency Mixing for Pulsed ns Ti:Sapphire Laser Systems at On-Line Radioactive Ion Beam Facilities, in: Proceedings of the Conference on Advances in Radioactive Isotope Science (ARIS2014), id.030126, 2015, p. 030126. doi:10.7566/JPSCP.6.030126.

[12] M. Santos, J. Marçalo, A. P. de Matos, J. K. Gibson, R. G. Haire, Gas-phase oxidation reactions of neptunium and plutonium ions investigated via fourier transform ion cyclotron resonance mass spectrometry, The Journal of Physical Chemistry A 106 (31) (2002) 7190–7194.

[13] T. Su, M. T. Bowers, Chapter 3 - classical ion–molecule collision theory, in: M. T. Bowers (Ed.), Gas Phase Ion Chemistry, Academic Press, 1979, pp. 83 – 118.

[14] K. Hiraoka, Gas-phase ion/molecule reactions, in: K. Hiraoka (Ed.), Fundamentals of Mass Spectrometry, Springer New York, 2013, pp. 109–144.

[15] I. Pohjalainen, I. D. Moore, T. Eronen, A. Jokinen, H. Penttilä, S. Rinta-Antila, Gas purification studies at IGISOL-4, Hyperfine Interactions 227 (1-3) (2014) 169–180.

[16] P. N. Johnston, P. A. Burns, Absolute L X-ray intensities in the decays of 230Th, 234U, 238Pu and 244Cm , Nuclear Instruments and Methods in Physics Research Section A: Accelerators, Spectrometers, Detectors and Associated Equipment 361 (1–2) (1995) 229 – 239.

[17] M. Lépy, B. Duchemin, J. Morel, Comparison of experimental and theoretical L X — ray emission probabilities of 241Am, 239Pu and 240Pu, Nuclear Instruments and Methods in Physics Research Section A: Accelerators, Spectrometers, Detectors and Associated Equipment 353 (1–3) (1994) 10 – 15.

[18] V. P. Chechev, The Evaluation of 238Pu, 240Pu, and 242Pu Decay Data, AIP Conference Proceedings 769 (1) (2005) 91–94.

[19] T. Kessler, I. Moore, Y. Kudryavtsev, K. Peräjärvi, A. Popov, P. Ronkanen, T. Sonoda, B. Tordoff, K. Wendt, J. Äystö, Off-line studies of the laser ionization of yttrium at the IGISOL facility, Nuclear Instruments and Methods in Physics Research Section B: Beam Interactions with Materials and Atoms 266 (4) (2008) 681 – 700.

[20] National Nuclear Data Center, information extracted from the Chart of Nuclides database, accessed: 2015-09-01.
URL `http://www.nndc.bnl.gov/chart/`